

Photovoltaic MPPT Tracking under Partial Shading Based on ICS-IGSS-INC Hybrid Algorithm

Tan Liu, Hexu Yu, Sisi Liu, Jiaqi Tong, Zhiyi Wu, Qingyun Yuan

Abstract—The P-V characteristic curve of a photovoltaic array exhibits several peaks in conditions of partial shade. Accurately tracking the Global Maximum Power Point (GMPP) of the complete photovoltaic system array is challenging since traditional Maximum Power Point Tracking (MPPT) methods frequently fall into the Local Maximum Power Points (LMPP). Although MPPT control methods based on intelligent optimization algorithms have been widely adopted to address this issue, balancing tracking accuracy and speed remains a challenging problem. A hybrid MPPT control strategy based on Improved Cuckoo Search-Golden Section Search in conjunction with the Incremental Conductance Method (ICS-IGSS-INC) is suggested in order to swiftly and precisely track the GMPP under partial shade conditions. The ICS algorithm is employed for global optimization, while IGSS and INC are used for local optimization, which enhances the accuracy and speed of the control algorithm. Simulation results indicate that compared with Particle Swarm Optimization (PSO), Cuckoo Search (CS), Improved Cuckoo Search (ICS), and Improved Cuckoo Search combined with Incremental Conductance (ICS-INC), the proposed ICS-IGSS-INC MPPT method significantly improves accuracy and speed, reduces power oscillations during tracking, and accurately tracks GMPP.

Index Terms—GMPP tracking; improved cuckoo algorithm; improved golden section algorithm; partial shading.

I. INTRODUCTION

ENERGY is a fundamental pillar for social progress and economic development. With population growth and economic development, the total energy consumption has

been increasing year by year [1]. Simultaneously, the environmental pollution caused by fossil fuels is becoming increasingly serious, making environmental protection and renewable clean energy a focus of current research. Among renewable energy sources, solar energy is widely recognized for its pollution-free, widely distributed, and low maintenance cost, and has received considerable attention both domestically and internationally [2]. However, photovoltaic power generation is easily affected by external environmental factors, resulting in low power generation efficiency. To address this issue, Maximum Power Point Tracking (MPPT) control technology has been developed [3]. Currently, MPPT control methods are mainly divided into traditional MPPT control and global MPPT control based on intelligent algorithms. The constant voltage method, incremental conductance method (INC), and perturbation observation method are the traditional methods of MPPT control [4-5]. When there is uniform illumination, these algorithms are able to track the Global Maximum Power Point (GMPP), but under partial shade, they often fall into the Local Maximum Power Points and cannot track GMPP. Intelligent optimization techniques, such as Particle Swarm Optimization (PSO) [6], Whale Optimization Algorithm (WOA) [7], and Cuckoo Search (CS) [8], are frequently used in MPPT control to boost the effectiveness of photovoltaic power generation under partial shade conditions.

In reference [9], PSO is combined with bacterial foraging for global optimization under partial shading, demonstrating that this combination method has superior global search capability. In reference [10], an improved sparrow search algorithm is suggested, which adjusts the step size by introducing dynamic variable rules and designs adaptive rules to update the discoverer's position. Thus, the search ability has been improved, and the algorithm effectively avoids local optima, enabling fast tracking of GMPP. In reference [11], the CS algorithm is combined with the Golden Section Search (GSS). Initially, the CS algorithm tracks the vicinity of GMPP, followed by the GSS algorithm for local optimization. According to simulation results, the combination algorithm enhances tracking efficiency and has a strong global search capability.

Although many MPPT control algorithms have been proposed, there is still room for improvement in tracking accuracy and speed. Therefore, a new MPPT control method based on Improved Cuckoo Search-Golden Section Search combined with Incremental Conductance Method (ICS-IGSS-INC) is proposed. First, the algorithm optimizes the initial population position of cuckoo birds and introduces an elite-guided cross-border processing mechanism, enhancing the global search ability. It conducts a large-scale

Manuscript received April 19, 2024; revised December 19, 2024. This work was supported by Liaoning provincial Education Department Project (LJKMZ20221035, LJKZ0683), Liaoning Provincial Science and Technology Department Project (2023-MS-212), National Natural Science Foundation of China (No. 32001415)

Tan Liu is an associate professor of School of Information and Electrical Engineering, Shenyang Agricultural University, Shenyang 110866, China (e-mail: liutan 0822@126.com).

Hexu Yu is a postgraduate student of School of Information and Electrical Engineering, Shenyang Agricultural University, Shenyang 110866, China (e-mail: 3173638014@qq.com).

Sisi Liu is a postgraduate student of School of Information and Electrical Engineering, Shenyang Agricultural University, Shenyang 110866, China (e-mail: 1737171700@qq.com).

Jiaqi Tong is an undergraduate student of School of Information and Electrical Engineering, Shenyang Agricultural University, Shenyang 110866, China (e-mail: 2936703706@qq.com).

Zhiyi Wu is a postgraduate student of School of Information and Electrical Engineering, Shenyang Agricultural University, Shenyang 110866, China (e-mail: 2579326790@qq.com).

Qingyun Yuan is an associate professor of School of Information and Electrical Engineering, Shenyang Agricultural University, Shenyang 110866, China (corresponding author, phone: 86-188098871409; e-mail: yqy8_29@126.com).

initial search to quickly find the approximate location of GMPP among multiple peaks under partial shading conditions, preventing the algorithm from falling into local optima. Then, variable step size is used to optimize the incremental conductance method and refine the parameters of the golden ratio algorithm. IGSS-INC is used for precise search of single peaks near GMPP, ensuring accurate tracking and location of GMPP. Simulation results demonstrate that the suggested method can track GMPP more quickly and minimize power oscillations in comparison to the original CS algorithm and other intelligent optimization techniques.

II. PHOTOVOLTAIC ARRAY PERFORMANCE UNDER COMPLEX SHADING CONDITIONS

A. Mathematical modeling of photovoltaic cells

In a photovoltaic power generation system, photovoltaic modules are composed of multiple series-parallel photovoltaic cells. Fig. 1 shows the photovoltaic modules' equivalent circuit diagram.

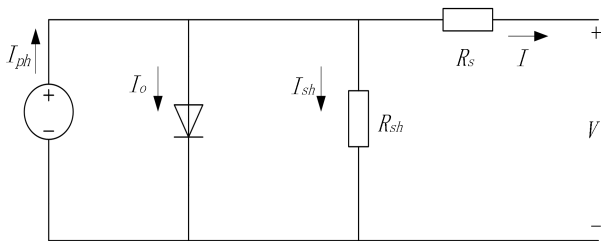


Fig. 1. Equivalent circuit of photovoltaic module

A photovoltaic module's output voltage and output current can be represented mathematically as follows:

$$I = I_{ph} - I_0 \left\{ \exp \left[\frac{q(V + IR_s)}{nkT} \right] - 1 \right\} - \frac{V + IR_s}{R_{sh}} \quad (1)$$

where I_{ph} denotes the photogenerated current, I_0 denotes the equivalent diode reverse saturation current, q represents the unit charge, n is the diode characteristic factor, k represents the Ludwig Boltzmann constant, T represents the temperature, R_{sh} represents the equivalent parallel resistance, R_s denotes the equivalent series resistance, V and I represent the output voltage and output current of the photovoltaic module, respectively. Among them, the resistance value of R_{sh} denotes approximately infinite, while the resistance value of R_s denotes very small and can be ignored. Therefore, Equation (1) can be expressed in a simplified form as follows:

$$I = I_{ph} - I_0 \left[\exp \left(\frac{qV}{nkT} \right) - 1 \right] \quad (2)$$

B. Multi-peak output characteristics of photovoltaic arrays

Four PV modules connected in series are utilized to simulate the multi-peak behavior of partially shaded PV output under three different operating conditions. The component parameters are set as: $U_{oc}=36.3V$, $I_{sc}=7.84A$, $P_{mpp}=213.15W$, $U_{mpp}=29V$, $I_{mpp}=7.35A$, the three conditions are: $[1000, 1000, 1000, 1000]$ W/m², $[1000, 1000, 800, 600]$ W/m², $[1000, 800, 600, 400]$ W/m², Fig. 2 displays the PV output's P-V characteristic curves under three distinct shadow distributions.

Fig. 2 shows that under uniform irradiance, the photovoltaic P-V characteristic curve contains only one GMPP. In contrast, under partial shading, there are multiple

LMPPs besides GMPP. In this case, using traditional MPPT control methods may cause the system to get stuck in LMPP, resulting in energy loss.

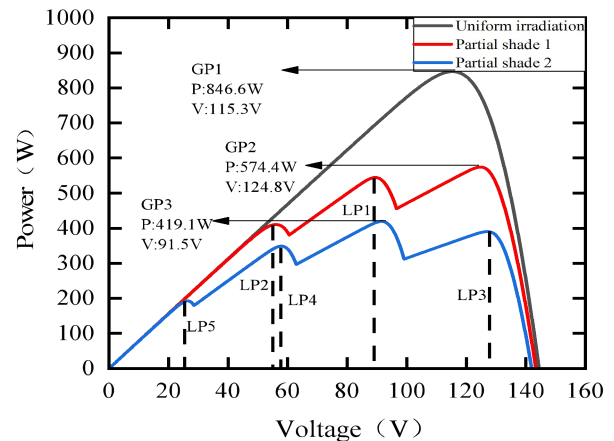


Fig. 2. PV array P-V curve under complex shading

Consequently, in conditions with partial shadowing, the MPPT control algorithm must employ global search techniques to bypass LMPP and accurately track GMPP, thereby improving the efficiency of photovoltaic power generation.

III. MPPT CONTROL USING THE ICS ALGORITHM

A. CS algorithm

The CS method is a clever optimization technique that was motivated by cuckoo bird nesting behavior [12-13]. In terms of optimization, cuckoos represent particles searching for solutions, and their eggs represent the solutions generated by the current iteration. The tracking process's random step size in CS algorithms adheres to a specific distribution property. Cuckoos are one of several natural species that exhibit random flight or movement, a characteristic feature of Lévy flight. This allows the CS algorithm to make "long jumps" during the search process by following the Lévy distribution for step sizes. This "leapfrogging" capability is essential for the CS algorithm, enabling it to prevent LMPP and decrease the time required to reach GMPP.

There are two ways to update positions in the CS search algorithm, including global Levy flight and local random walk. The likelihood that the host bird will discover the eggs when the cuckoo deposits them in the nest is P_a . If each nest corresponds to a random number r_i , and if $r_i > P_a$, the parasitic nest will be discovered and abandoned by the host. In this case, it is necessary to perform local random walks for updating the nested position at any time. The updated formula is expressed as follows:

$$x_i^{t+1} = x_i^t + r_i (x_j^t - x_k^t) \quad (3)$$

where t denotes the current iteration count, x_i^t denotes the position of the i -th bird's nest in the t -th iteration, x_j^t denotes the positions of two randomly chosen nests at iteration t .

The updated formula for Levi's overall flight is expressed as follows:

$$\begin{cases} x_i^{t+1} = x_i^t + \alpha \oplus L(\beta) \\ L(\beta) = \frac{u}{|v|^{1/\beta}} (x^t - x_{best}^t) \end{cases} \quad (4)$$

where α denotes the step size coefficient of Levis's flight, \oplus is the dot product, x_i^t is the position of the i -th bird during the t -th iteration, and x_{best}^t denotes the best parasitic nest in the iteration, $u \sim N(0, \sigma^2)$, $v \sim N(0, 1)$.

$$\sigma = \left[\frac{\Gamma(1+\beta) \sin(\pi\beta/2)}{\Gamma(\frac{1+\beta}{2}) \times \beta \times 2^{(\beta-1)/2}} \right]^{1/\beta} \quad (5)$$

where Γ represents the standard gamma function.

B. Improved CS algorithm

Due to the Cuckoo algorithm using Lévy flight search [14-15], the search process is often more random and lacks communication between nests. This may result in slower convergence speed and the algorithm getting stuck in LMPP. To address these issues, the Cuckoo algorithm has been improved as follows:

(1) Adaptive discovery probability and step size

P_a is the likelihood that the host bird will find the cuckoo; if P_a is too low, it will enter a local optima. When P_a is too high, the rate of convergence will decrease. In the standard cuckoo algorithm, $P_a=0.25$. This may lead to insufficient search accuracy in the early stages of the algorithm and an increase in the count of iterations in the later stage [16]. As the probability of discovery increases, the number of nested updates in each iteration of the algorithm further increases, thereby improving the accuracy of the optimization algorithm. Simultaneously, the algorithm's computational complexity has grown, making it more complex.

The cuckoo algorithm always optimizes towards the optimal direction during the optimization process, so that the cuckoo can avoid being found by the host bird and imitate its call, reducing the probability of being discovered.

Therefore, by selecting the adaptive change of P_a , the P_a value of the algorithm dynamically decreases from the initial phase to the later phase. The larger the initial value of P_a , the greater the capacity for worldwide search and the quicker the speed of convergence. The P_a value steadily drops as the count of iterations rises, and the algorithm's local search accuracy improves over time.

The improved P_a value is expressed as follows:

$$P_a = \frac{1}{\exp\left[\text{sqr}\left(\frac{t}{T}\right)\right]} - 0.25 \quad (6)$$

where t denotes the current number of iterations, and T denotes the maximum number of iterations. The range of P_a change is from 0.22 to 0.6.

(2) Adaptive step size coefficient

When the cuckoo flies use Lévy flight to find parasitic nests, the coefficient of step size will influence the search range, as shown in Equation (6). A larger step size will expand the search range, while a smaller step size will narrow the search range, thereby finding the best solution in a smaller area [17]. As a result, an adjustable step-size coefficient for Lévy flight is suggested for strengthening the algorithm's rate of convergence and global search capability. The following is how this coefficient is expressed:

$$\alpha = \frac{2\sin\left(\frac{\pi t}{2T} + \pi\right) \times \text{rand}(1)}{5} + 1 \quad (7)$$

(3) Optimization of the initial position of the population

To increase the tracking speed of global optimization, the original voltage range is improved by selecting 0.8 times the array open-circuit voltage U_{oc} as the initial voltage.

(4) Elite-guided cross-border treatment mechanism

The cuckoo will remain at the boundary value in the basic CS algorithm if it flies away from the established border while searching for the nest. The search range is somewhat constrained by this approach, but it takes several iterations to find the ideal boundary.

Therefore, in order to improve the algorithm's capacity for global search and rate of convergence, the boundary-crossing processing criteria are reset as follows:

$$X = X_{best} + \text{randsrc} * T / t * 2 \quad (8)$$

where T denotes the maximum number of iterations, t represents the current iteration count, X_{best} denotes the current optimal position, and randsrc denotes a uniformly distributed random number.

C. MPPT control using the ICS algorithm

The population's location on the P-V characteristic curve of the PV output utilized for maximum power tracking corresponds to the voltage position under local shading conditions in MPPT control based on the ICS algorithm. To determine the output power, the controller measures the corresponding photovoltaic output's voltage and current. A larger population size leads to higher accuracy in identifying peak power but also increases computation time. The count of iterations is set to 10, and the count of cuckoos is set to 5 in order to balance computation time and accuracy.

The output power of a photovoltaic system varies with the intensity of light. The condition for restarting the ICS algorithm is determined by sensing the change in output power, as described in Equation (9).

$$\left| \frac{P^k - P^{k-1}}{P^k} \right| \geq 0.05 \quad (9)$$

where P^k denotes the current power value, and P^{k-1} denotes the power value of the last cycle.

Fig. 3 displays the block diagram of the ICS-based photovoltaic MPPT control system. Among them, $C_1=20\mu\text{F}$, $L=0.003\text{mH}$, $C_2=200\mu\text{F}$, and $R_{load}=50\Omega$, the number, parameters, and operating conditions of PV modules are shown in Section II.

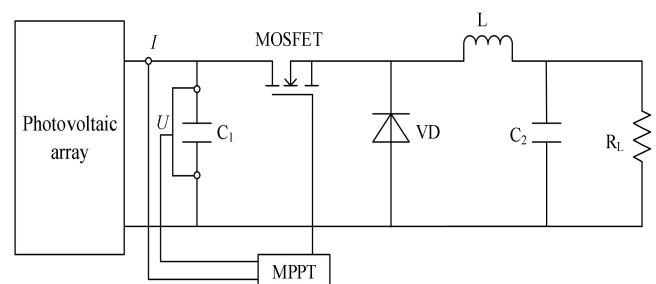


Fig. 3. Block diagram of photovoltaic MPPT control system

D. Simulation comparison based on ICS algorithm

The MPPT simulation results of PSO, CS, and ICS under three different operating conditions are compared. Fig. 4 displays the MPPT comparison results under uniform irradiation.

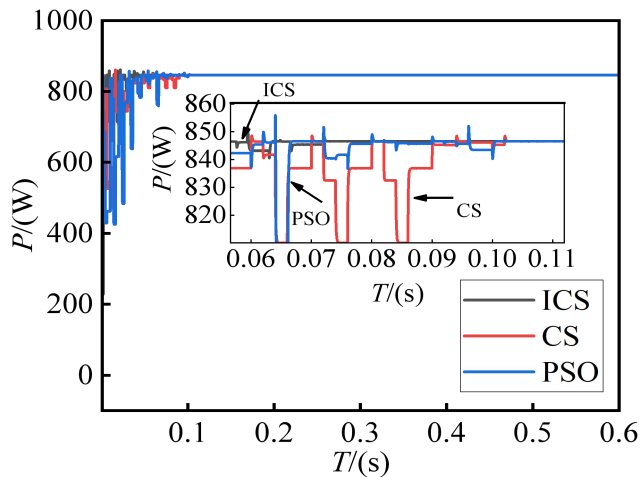


Fig. 4. Power waveform tracked by algorithm under condition 1

According to Fig. 4, the PSO algorithm has a 99.96% tracking efficiency, a tracking time of 0.11s, and an inaccuracy of 0.3 W for GMPP-846.3W. The CS algorithm has a 99.94% tracking efficiency, a tracking time of 0.10s, and an inaccuracy of 0.5 W for GMPP-846.1 W. For GMPP-846.6 W, on the other hand, the ICS algorithm achieves 100% tracking efficiency with a tracking duration of just 0.07s. The PSO and CS algorithms require more tracking time, bigger power oscillations, and lower tracking efficiency when compared to the ICS method, as shown in Fig. 4. The ICS algorithm demonstrates faster convergence speed, stronger optimization ability, and more stable maximum power output under uniform irradiance conditions.

MPPT simulations are performed on PSO, CS, and ICS algorithms under condition 2, and Fig. 5 displays the MPPT comparison findings.

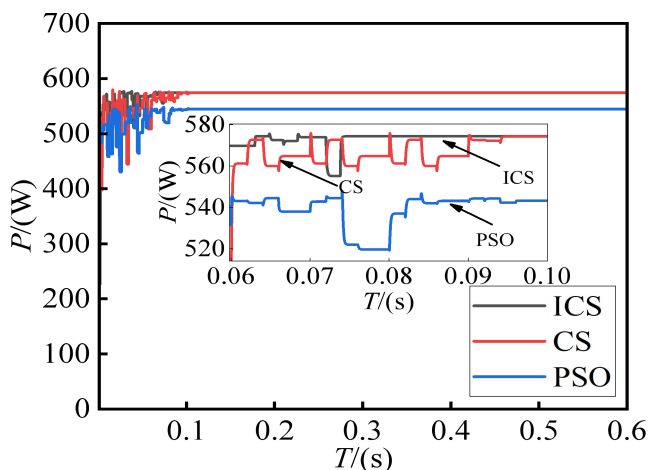


Fig. 5. Power waveform tracked by algorithm under condition 2

Fig. 5 shows that the PSO algorithm achieves a tracking efficiency of 94.76% and a tracking time of 0.104s for GMPP-544.3W. With a tracking effectiveness of 99.13%, the CS algorithm has a tracking time of 0.096s for GMPP-569.4W. The tracking effectiveness of the ICS algorithm is 99.97%, and its tracking time for the

GMPP-574.2W is 0.082s. The ICS algorithm exhibits faster convergence speed, stronger optimization ability, and more stable maximum power output under local shading conditions.

Fig. 6 displays the MPPT comparison findings under condition 3. It is evident that the PSO algorithm has a 99.45% tracking efficiency and a tracking time of 0.1s for GMPP-416.8 W. For GMPP-418.6 W, the CS algorithm's tracking time is 0.102s, and its tracking efficiency is 99.88%. For GMPP-418.7 W, the ICS algorithm's tracking time is 0.081s, and its tracking efficiency is 99.90%. That is to say, the ICS algorithm achieves the best results.

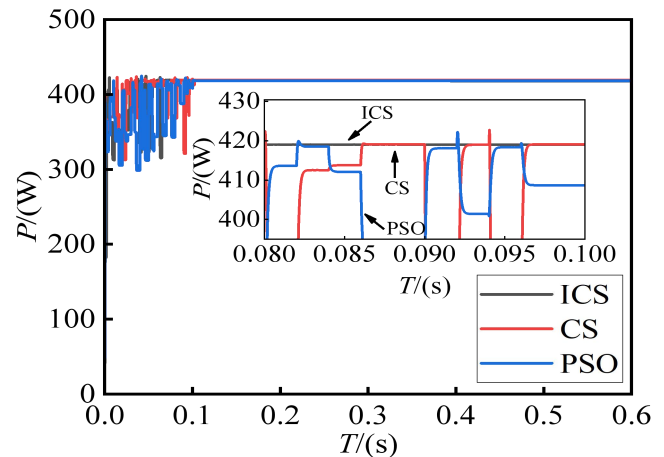


Fig. 6. Power waveform tracked by algorithm under condition 3

Under all irradiance conditions, the ICS algorithm exhibits better convergence time, higher tracking efficiency, and stronger searchability, as shown in Table 1. Furthermore, the maximum output power is more consistent, which results in the highest tracking efficiency overall.

TABLE I
PERFORMANCE COMPARISON OF THREE ALGORITHMS

Conditions	Algorithm	P/W	t/s	$\eta/\%$
Condition 1	PSO	846.3	0.110	99.96
	CS	846.1	0.100	99.94
	ICS	846.6	0.079	100.00
Condition 2	PSO	544.3	0.104	94.76
	CS	569.4	0.096	99.13
	ICS	574.2	0.082	99.97
Condition 3	PSO	416.8	0.100	99.45
	CS	418.6	0.102	99.88
	ICS	418.7	0.082	99.90

IV. MPPT CONTROL BASED ON ICS-IGSS-INC

A. GSS algorithm

One technique for handling optimization issues involving single-hump functions is the GSS algorithm [18–19]. GSS is applied to address the single-peak MPPT issue in reference [20]. The GSS algorithm covers a tracking region first, then progressively reduces that area until it converges to the maximum point to find the maximum point. The algorithm's main concept is to pinpoint the maximum point precisely by using the "Golden Ratio" technique to properly narrow the monitoring region.

The following specifications must be fulfilled by the insertion site in order to maximize the tracking process.

$$\frac{V_{g3} - V_{g1}}{V_{g4} - V_{g1}} = \frac{V_{g4} - V_{g2}}{V_{g4} - V_{g1}} = 0.618 \quad (10)$$

B. IGSS algorithm

In each iteration, the golden ratio in the search interval is used to find the extremum of a unary function within a given interval [21]. From the point of view of mathematics, this ratio shortens the interval by 0.51. As a result, the algorithm's tracking time and optimization speed are able to be further enhanced.

The proposed IGSS is essentially an improvement on GSS. By reducing the shortening rate of each search from 0.618 to 0.51, the interval after each search is reduced to 0.51 times that of the previous search. Compared with the GSS algorithm, this significantly increases the tracking speed. As a result, the proposed IGSS can successfully raise photovoltaic power generation efficiency.

C. MPPT control strategies utilizing ICS-IGSS-INC hybrid algorithm

The primary concept of the ICS-IGSS-INC hybrid algorithm-based MPPT control approach is to enhance the tracking speed of photovoltaic MPPT by combining the ICS, IGSS, and INC algorithms and leveraging their benefits. To

identify the area where the GMPP is situated, four ICS algorithm particles are first sent out. The IGSS and INC algorithms are then triggered to precisely search for GMPP when the correct region has been determined.

The key strategy is to switch to faster IGSS and INC algorithms after identifying a specific region, thereby accelerating the tracking speed of the algorithm. To decide when the system should transition from ICS to IGSS, a suitable transition mechanism is needed. When designing this transition mechanism, certain rules will be employed to switch algorithms. In the proposed method, if ICS produces good results, the system will continue to use the ICS algorithm [22]. Otherwise, the system will switch to IGSS and INC, and the acceptable probability is defined as follows:

$$Acc_1 = \exp\left(\frac{\Delta P_1}{T}\right) = \exp\left(\frac{P_{ave} - P_{max}}{T}\right) \quad (11)$$

where ΔP_1 represents the discrepancy between the ideal outcome and the mean of all particles deployed. Since ICS uses several particles to look for GMPP, it is helpful to think of each particle as a representation of the system's current state. Fig. 7 displays the flow of MPPT control based on ICS-IGSS-INC hybrid algorithm .

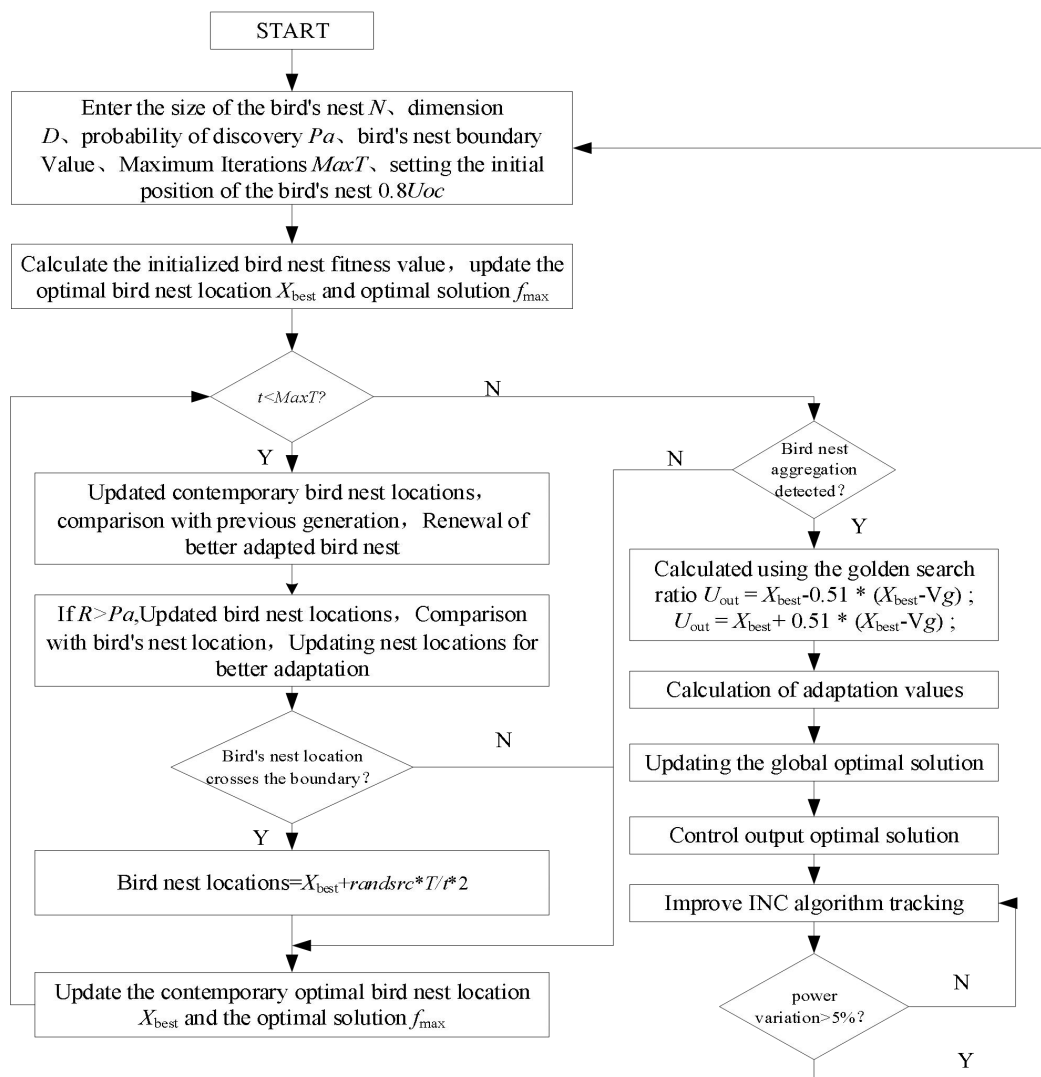


Fig. 7. MPPT control flow based on ICS-IGSS-INC

(1) Set the algorithm's starting parameters as follows: N denotes the population size, D denotes the count of dimensions, P_a represents the discovery probability, $MaxT$ denotes the maximum count of iterations, and $0.8Uoc$ denotes the beginning test position for nesting.

(2) After determining the first nest fitness value, update the optimal solution f_{max} and the ideal nest position X_{best} .

(3) Verify whether the current iteration t is less than the maximum count of iterations $MaxT$: If $MaxT > t$, Update the bird's nest to be more adaptive than the prior generation.

(4) If $R > P_a$: Update the nest with better adaptability compared to the previous generation.

(5) Verify whether the bird's nest is outside of the allowed area. If not, update the ideal bird's nest location X_{best} and the ideal solution f_{max} ; otherwise, update the ideal bird's nest using Equation (6).

(6) If t exceeds the maximum number of iterations, bird's nest aggregation is detected, and if bird's nest aggregation satisfies the probability acceptance level in Equation (11), IGSS-INC is used for local optimization and the maximum power is output.

(7) If nest aggregation is not detected, return to step (5).

(8) If a power difference before and after detection is greater than 5%, return to step (1).

D. Simulation comparison based on ICS-IGSS-INC hybrid algorithm

To verify the tracking effect of MPPT using the ICS-IGSS-INC hybrid algorithm, a 1×4 PV array simulation model is built. The model is used to compare the ICS-INC and ICS algorithms under the same irradiance. The parameters and circuit models of the photovoltaic MPPT control system have been introduced in detail in Section III.

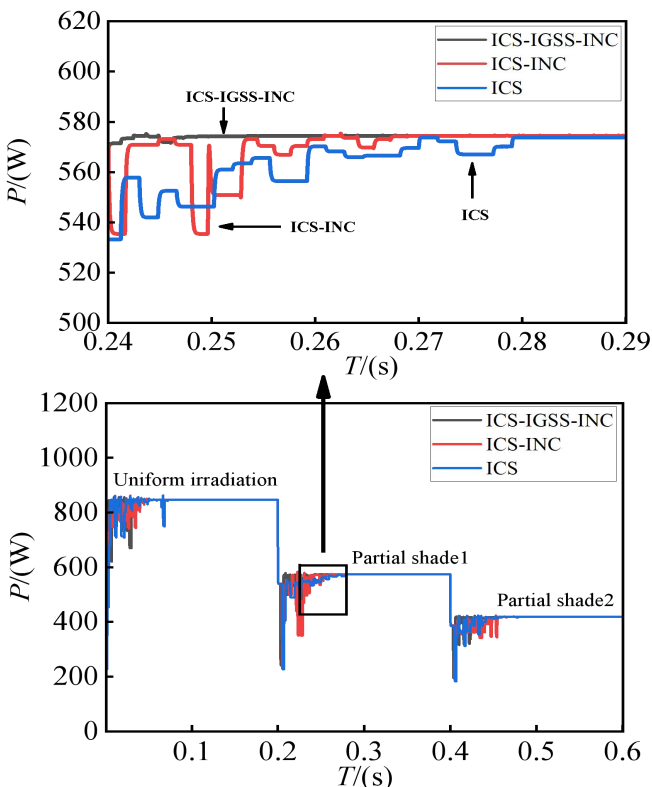


Fig. 8. Power waveforms tracked by three algorithmic

Under variable conditions, the hybrid algorithm based on ICS-IGSS-INC is simulated and compared with ICS and ICS-INC algorithms. Table 2 compares the three algorithms' performances, and Fig. 8 displays the MPPT comparison findings under uniform illumination.

As displayed in Fig. 8 and Table 2, the ICS-IGSS-INC hybrid algorithm requires 0.031s to track the GMPP at 846.6W, resulting in a tracking efficiency of 100.00%. The ICS-INC algorithm also tracks the GMPP at 846.6W but it requires 0.077s. Compared with the ICS-IGSS-INC hybrid algorithm, the ICS-INC algorithm takes 0.046s longer and exhibits a larger early oscillation amplitude. The ICS algorithm achieves a maximum power of 846.6W in 0.074s, demonstrating a tracking efficiency of 100.00%. The ICS algorithm has a greater power oscillation amplitude and takes 0.043s more time than the ICS-IGSS-INC hybrid algorithm.

From uniform irradiation to the first type of partial shading condition, the hybrid ICS-IGSS-INC algorithm tracks GMPP at 574.4W within 0.044s, with a tracking efficiency of 100.00% and very low power oscillation amplitude. The ICS-INC algorithm tracks GMPP at 573.8W, achieving a tracking efficiency of 99.90% and taking 0.061s. Compared with the hybrid ICS-IGSS-INC algorithm, the ICS-INC algorithm requires 0.017s more time and has a greater power oscillation amplitude. The ICS algorithm takes 0.089s to track GMPP at 573.1W, with a tracking efficiency of 99.77%. Compared with the hybrid ICS-IGSS-INC algorithm, the ICS algorithm requires 0.045s more time and exhibits a larger power oscillation amplitude.

TABLE II
PERFORMANCE COMPARISON OF THREE ALGORITHMS

Conditions	Algorithm	P/W	t/s	$\eta/\%$
Condition 1	ICS	846.6	0.074	100.00
	ICS-INC	846.6	0.077	100.00
Condition 2	ICS-IGSS-INC	846.6	0.031	100.00
	ICS	573.1	0.089	99.77
	ICS-INC	573.8	0.061	99.90
Condition 3	ICS-IGSS-INC	574.4	0.044	100.00
	ICS	418.7	0.082	99.90
	ICS-INC	419.0	0.080	99.98
	ICS-IGSS-INC	419.1	0.039	100.00

Upon converting the first partial shading type to the second partial shading type, the hybrid ICS-IGSS-INC algorithm achieves a tracking efficiency of 100.00% by tracking the GMPP at 419.1W in 0.039 s. The ICS-INC algorithm tracks the GMPP at 419.0W within 0.080s, with a tracking efficiency of 99.98%. Compared with the hybrid ICS-IGSS-INC algorithm, the ICS-INC algorithm takes 0.041s longer and shows a greater power oscillation amplitude. The tracking effectiveness of the ICS algorithm is 99.90%, and it takes 0.082 s to track the GMPP at 418.7W. In comparison to the ICS-IGSS-INC hybrid algorithm, the ICS algorithm has a greater power oscillation amplitude and requires 0.043s more time.

V. EXPERIMENTAL VERIFICATION

As seen in Fig. 9, an experimental platform for photovoltaic MPPT control is constructed in order to confirm the algorithm's validity and viability.



Fig. 9. Photovoltaic MPPT control experimental platform

The experimental platform incorporates an MPPT controller and simulates the output of a photovoltaic using a photovoltaic analog source with a resistance acting as the load. MPPT control under partial shade conditions is simulated by setting the P-U characteristic curve as illustrated in Fig. 10. Three conditions are [1000, 1000, 1000] W/m², [1000, 1000, 400] W/m², and [1000, 600, 400] W/m², respectively. The experiment process is as follows: uniform irradiation is switched to local shading 1, and then local shading 1 is switched to local shading 2. As shown in Fig. 10, during the switching process, the voltage position of the maximum power point shifts, starting from 51.2V, moving to 33.2V, and finally reaching 55.7V.

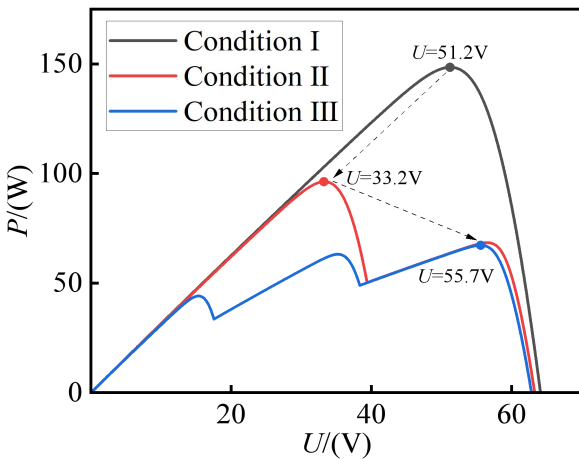


Fig.10. Characteristic curves for P-U in three distinct scenarios

Figs. 11–13 display the photovoltaic analog source's output voltage changes for the ICS-IGSS-INC, ICS-INC, and ICS algorithms during the tracking process, respectively.

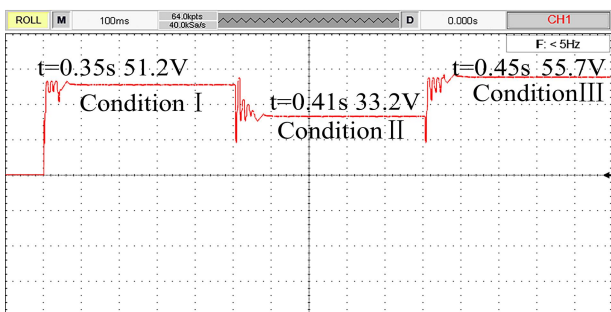


Fig.11. Output voltage controlled by ICS-IGSS-INC algorithm

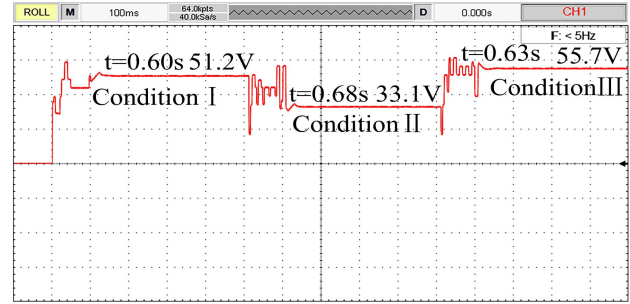


Fig.12. Output voltage controlled by ICS-INC algorithm

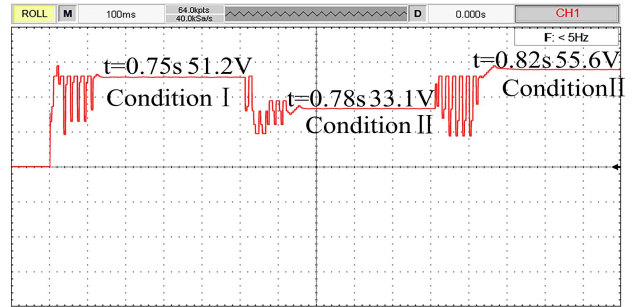


Fig.13. Output voltage controlled by ICS algorithm

In these figures, the abscissa represents time and the ordinate represents output voltage. It can be observed that the tracking process of the ICS-IGSS-INC algorithm is very fast and smooth, with minimal overall fluctuations.

TABLE III
PERFORMANCE COMPARISON OF THREE ALGORITHMS

Conditions	Algorithm	U/V	t/s	$\eta/\%$
Condition 1	ICS	51.2	0.75	100.00
	ICS-INC	51.2	0.6	100.00
	ICS-IGSS-INC	51.2	0.35	100.00
Condition 2	ICS	33.1	0.78	99.70
	ICS-INC	33.1	0.68	99.70
	ICS-IGSS-INC	33.2	0.41	100.00
Condition 3	ICS	55.6	0.82	99.82
	ICS-INC	55.7	0.63	100.00
	ICS-IGSS-INC	55.7	0.45	100.00

Furthermore, Table 3 shows that, under condition 1, the ICS algorithm tracks to the maximum power point in 0.75 s with a 100% tracking efficiency, the ICS-INC algorithm tracks to the maximum power point in 0.6 seconds with a 100% tracking efficiency, and the ICS-IGSS-INC algorithm tracks to the maximum power point in 0.35 seconds with a 100% tracking efficiency. These algorithms significantly reduce the tracking time. Under condition 2, the ICS algorithm tracks the maximum power point in 0.78 seconds with a 99.7% tracking efficiency, the ICS-INC algorithm tracks the maximum power point in 0.68 s with a 99.7% tracking efficiency, and the ICS-IGSS-INC algorithm tracks the maximum power point in 0.41 s, significantly cutting down on tracking time and reaching a 100% tracking efficiency. The ICS algorithm takes 0.82 s with a 99.82% tracking efficiency to track the maximum power point under condition 3, the ICS-INC algorithm takes 0.63 seconds with a 100% tracking efficiency, and the ICS-IGSS-INC algorithm takes 0.45 s with a 100% tracking efficiency and smaller oscillations, significantly cutting down on tracking time. It is evident that the ICS-IGSS-INC, ICS-INC, as well as the

capability of ICS algorithms to track near the maximum power point. The ICS-IGSS-INC algorithm is the fastest with regard to tracking quickness and effectiveness, with the ICS-INC algorithm coming in second. The ICS algorithm is the slowest. This indicates further that the suggested algorithm has strong robustness and acceptable dynamic quality.

VI. CONCLUSION

Aiming at the multi-peak characteristic of PV output under partial shade conditions and the slow convergence speed of the CS algorithm, an ICS-IGSS-INC hybrid algorithm is proposed and applied to MPPT control. The main conclusions are as follows:

Improved tracking efficiency: the ICS algorithm achieves a tracking efficiency of 99.90%, outperforming the CS and PSO algorithms, with a convergence time of just 0.082 seconds in sudden illumination conditions. This approach minimizes the risk of local optima and enhances tracking performance.

Enhanced performance of hybrid algorithm: By comparing the maximum power tracked by ICS and ICS-INC algorithms, the hybrid ICS-IGSS-INC algorithm achieves a tracking efficiency of 100.00%. During the convergence process, this hybrid method lowers power oscillation and increases tracking efficiency.

Robustness and dynamic quality: Simulation results show that MPPT based on the ICS-IGSS-INC hybrid algorithm can effectively handle environmental uncertainties such as illumination changes. It quickly and stably searches for global GMPP, thereby improving the maximum power tracking efficiency of photovoltaic power generation systems under uncertain situations.

The proposed algorithm is validated through a physical simulation platform, with results indicating that the ICS-IGSS-INC algorithm can rapidly track the maximum power point while reducing power oscillations during convergence. This further confirms the algorithm's strong dynamic performance and robustness.

REFERENCES

- [1] A. J. Salim, B. M. Albaker, S. M. Alwan, and M. Hasanuzzaman, "Hybrid MPPT approach using cuckoo search and grey wolf optimizer for PV systems under variant operating conditions," *Global Energy Interconnection*, vol. 5, no. 6, pp. 627-644, 2022.
- [2] L. Q. Shang, and F. Li, "PV power point tracking based on adaptive cuckoo search and perturbation observation method," *Power System Protection and Control*, vol. 50, no. 8, pp. 99-107, 2022.
- [3] L. M. Wei, and Y. Y. Wu, "Research on MPPT algorithm of photovoltaic array under complex illumination," *Chinese Journal of Power Sources*, vol. 46, no. 6, pp. 688-692, 2022.
- [4] S. X. Mo, Q. T. Ye, K. P. Jiang, X. F. Mo, and G. Y. Shen, "An improved MPPT method for photovoltaic systems based on mayfly optimization algorithm," *Energy Reports*, vol. 8, pp. 141-150, 2022.
- [5] L. K. Guo, D. Yan, and J. Z. Fu, "MPPT research of photovoltaic system based on improved perturbation observation method," *Chinese Journal of Power Sources*, vol. 45, no. 1, pp. 56-59, 2021.
- [6] S. Javed, and K. Ishaque, "A comprehensive analysis with new findings of different PSO variants for MPPT problem under partial shading," *Ain Shams Engineering Journal*, vol. 13, no. 5, pp. 101680, 2022.
- [7] H. Z. Wu, and X. Gao, "Research on MPPT of photovoltaic array with improved whale optimization algorithm under partial shading conditions," *Journal of Jiamusi University (Natural Science Edition)*, vol. 40, no. 5, pp. 12-15, 2022.
- [8] C. J. Ge, P. Wu, X. X. Dong, J. Z. Jin, "Improved photovoltaic maximum power point tracking based on cuckoo search algorithm," *Acta Energetica Solaris Sinica*, vol. 43, no. 10, pp. 59-64, 2022.
- [9] Z. Hao, J. D. Zhang, C. R. Huang, and Z. A. Xue, "Application of hybrid algorithm of particle swarm optimization and bacterial foraging in MPPT of photovoltaic system," *Electrotechnics Electric*, no. 6, pp. 14-19, 2021.
- [10] Q. W. Fang, H. P. Liu, M. Wang, G. Q. Li, X. Dong, "Application of Improved Sparrow Search Algorithm in Photovoltaic Arrays MPPT," *Electric Machines & Control Application*, vol. 49, no. 7, pp. 87-94+103, 2022.
- [11] D. A. Nugraha, K. L. Lian, "A novel MPPT method based on cuckoo search algorithm and golden section search algorithm for partially shaded PV system," *Canadian Journal of Electrical and Computer Engineering*, vol. 42, no. 3, pp. 173-182, 2019.
- [12] S. Q. Zhao, H. Xiao, and Z. B. Liu, "Photovoltaic maximum power point tracking under partial shading based on CSA-IP&O," *Power System Protection and Control*, vol. 48, no. 5, pp. 26-32, 2020.
- [13] Y. Xu, "Application of improved particle swarm optimization in distribution network reconfiguration with distributed generation," *Electrical Measurement & Instrumentation*, vol. 58, no. 3, pp. 98-104, 2021.
- [14] X. Q. Xu, B. Wang, and H. S. Zhao, "Reconfiguration of two-voltage distribution network based on cuckoo search and simulated annealing algorithm," *Power System Protection and Control*, vol. 48, no. 11, pp. 84-91, 2020.
- [15] W. Wongsinlatam, S. Buchitchon, "Criminal cases forecasting model using a new intelligent hybrid artificial neural network with cuckoo search algorithm," *IAENG International Journal of Computer Science*, vol. 47, no. 3, pp. 481-490, 2020.
- [16] L. Chen, S. C. Zheng, Y. Q. Jiang, H. K. Chen, and J. G. Tang, "Identifying multi-machine equivalent parameters of wind farms based on an improved chaotic cuckoo search algorithm," *Power System Protection and Control*, vol. 51, no. 20, pp. 100-106, 2023.
- [17] Y. H. Zhang, Y. F. Liu, X. H. Zhang, "A variable stepsize sparsity adaptive matching pursuit algorithm," *IAENG International Journal of Computer Science*, vol. 8, no. 3, pp. 770-775, 2021.
- [18] H. H. Mostafa, A. M. Ibrahim, and W. R. Anis, "A performance analysis of a hybrid golden section search methodology and a nature-inspired algorithm for MPPT in a solar PV system," *Archives of electrical engineering*, pp. 611-627, 2019.
- [19] H. Bahri, and A. Harrag, "Ingenious golden section search MPPT algorithm for PEM fuel cell power system," *Neural Computing and Applications*, vol. 33, no. 14, pp. 8275-8298, 2021.
- [20] J. Cheng, "Research on adaptive cuckoo algorithm and its application," *Lanzhou University*, 2021.
- [21] H. Y. Liu, "Research on MPPT Algorithm Based on Improved Golden Section Search and Realization," *Anhui University of Technology and Science*, 2016.
- [22] D. A. Nugraha, and K. L. Lian, "A novel MPPT method based on cuckoo search algorithm and golden section search algorithm for partially shaded PV system," *Canadian Journal of Electrical and Computer Engineering*, vol. 42, no. 3, pp. 173-182, 2019.

Tan Liu was born in Kaiyuan, Liaoning Province, China in 1985. He received the B.S. Degree and the M. S. degree from University of Science and Technology Liaoning, Liaoning, China in 2008 and 2011, respectively, majoring in automation and control theory and control engineering respectively. He received the PhD degree from Northeastern University, Liaoning, China in 2016 in control theory and control engineering. His main interests are photovoltaic power generation technology, environmental regulation and intelligent equipment in facility agriculture.